LETTER

doi:10.1038/nature10138

CCL2 recruits inflammatory monocytes to facilitate breast-tumour metastasis

Bin-Zhi Qian[1], Jiufeng Li[1], Hui Zhang[1], Takanori Kitamura[1], Jinghang Zhang[2], Liam R. Campion[3], Elizabeth A. Kaiser[3], Linda A. Snyder[3] & Jeffrey W. Pollard[1]

Macrophages, which are abundant in the tumour microenvironment, enhance malignancy[1]. At metastatic sites, a distinct population of metastasis-associated macrophages promotes the extravasation, seeding and persistent growth of tumour cells[2]. Here we define the origin of these macrophages by showing that Gr1-positive inflammatory monocytes are preferentially recruited to pulmonary metastases but not to primary mammary tumours in mice. This process also occurs for human inflammatory monocytes in pulmonary metastases of human breast cancer cells. The recruitment of these inflammatory monocytes, which express CCR2 (the receptor for chemokine CCL2), as well as the subsequent recruitment of metastasis-associated macrophages and their interaction with metastasizing tumour cells, is dependent on CCL2 synthesized by both the tumour and the stroma. Inhibition of CCL2–CCR2 signalling blocks the recruitment of inflammatory monocytes, inhibits metastasis *in vivo* and prolongs the survival of tumour-bearing mice. Depletion of tumour-cell-derived CCL2 also inhibits metastatic seeding. Inflammatory monocytes promote the extravasation of tumour cells in a process that requires monocyte-derived vascular endothelial growth factor. *CCL2* expression and macrophage infiltration are correlated with poor prognosis and metastatic disease in human breast cancer[3–6]. Our data provide the mechanistic link between these two clinical associations and indicate new therapeutic targets for treating metastatic breast cancer.

To understand the origin of macrophages in primary tumours and their metastatic sites, we measured monocyte trafficking. Mouse monocytes were identified by their expression of CD11b and CD115 (Supplementary Fig. 3a) and were sorted by fluorescence-activated cell sorting (FACS) into sub-populations of inflammatory monocytes expressing Gr1 and Ly6c and resident monocytes lacking Gr1 and Ly6c (refs 7, 8) (Supplementary Fig. 3b–d). Both populations had similar expression of GFP in *Csf1r–GFP* transgenic mice (Supplementary Fig. 3b). We adoptively transferred[9–11] 10^5 cells of each population into syngeneic FVB mice bearing autochthonous late-stage Polyoma Middle T (PyMT) mammary tumours with spontaneous pulmonary metastases (Fig. 1a). Eighteen hours after adoptive transfer, we determined the ratio of recovered GFP-positive inflammatory monocytes (Supplementary Fig. 3e) to resident monocytes from the same donor, to measure their relative recruitment. This indicated that there were similar numbers of donor cells in the blood (showing equivalent availability), but that in the primary tumour, resident monocytes were preferentially recruited, whereas in pulmonary metastases, inflammatory monocytes were preferentially recruited, with more than three-fold enrichment (Fig. 1b). Consistent with this, a notable population of endogenous inflammatory monocytes was identified in metastasis-bearing lungs but not in normal lungs (Supplementary Fig. 4a). This preferential recruitment of inflammatory monocytes in the lung was not observed in 7-week-old PyMT mice bearing pre-metastatic mammary tumours (Supplementary Fig. 4b). In experimentally induced pulmonary foci of intravenously injected Met-1 cells (a PyMT-induced mouse mammary tumour cell line)[12], inflammatory monocytes were also preferentially recruited (Supplementary Fig. 4c). GFP-labelled cells were readily detectable in pulmonary metastases at least 5 d after transfer (data not shown) and within 2 d, a significant portion of them had differentiated into $F4/80^+\,CD11b^+\,Gr1^-$ metastasis-associated macrophages (MAMs)[2] that are not seen in normal lungs (Supplementary Fig. 4d). To test whether inflammatory monocytes were recruited early in the metastasis process, we transferred monocyte populations

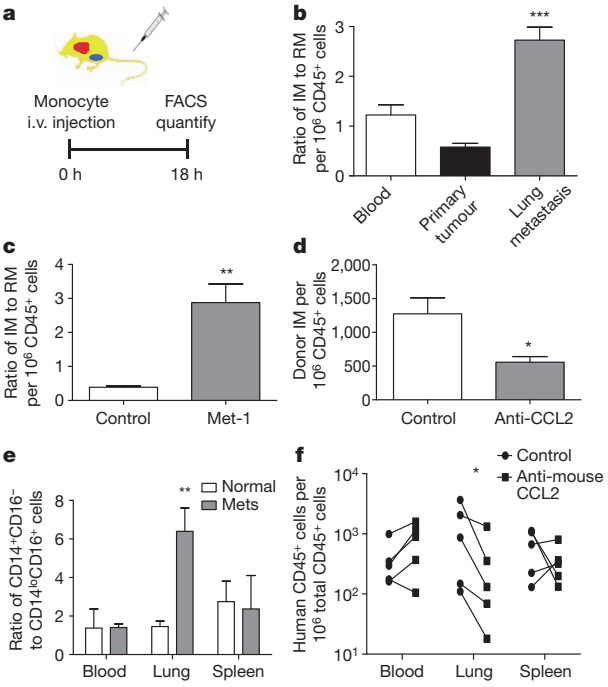

Figure 1 | Pulmonary metastases preferentially recruit inflammatory monocytes through CCL2. a, Schematic for the adoptive transfer of monocytes into PyMT-tumour-bearing mice with pulmonary metastases. i.v., intravenous. **b**, Ratios of inflammatory monocytes (IM) to resident monocytes (RM) in different tissues of recipient mice bearing PyMT tumours and metastases. $n = 6$; ***, $P < 0.0001$. **c**, Ratios of inflammatory monocytes to resident monocytes in control lungs and in lungs with Met-1 cells intravenously injected 7 h before measurement. $n = 4$; **, $P = 0.0039$. **d**, Relative numbers of donor inflammatory monocytes recruited in lungs challenged with Met-1 cells for 7 h, with control or anti-mouse CCL2 antibody treatment. $n = 3$; *, $P = 0.045$. **e**, Ratios of adoptively transferred $CD14^+CD16^-$ and $CD14^{low}CD16^+$ human monocytes recruited into the lungs of normal mice (open bars) and of mice challenged with 4173 cells that contain metastases (Mets: solid bars) for 7 h. $n = 5$; **, $P = 0.0163$. All bars show mean + s.e.m. **f**, Numbers of adoptively transferred human $CD14^+CD16^-$ monocytes that migrated into different tissues of mice challenged with 4173 cells via intravenous injection, with control or anti-mouse CCL2 antibody treatment. Each line connects data from the same donor. $n = 5$; *, $P = 0.016$.

[1]Department of Developmental and Molecular Biology, Center for the Study of Reproductive Biology and Women's Health, Albert Einstein College of Medicine, New York, New York 10461, USA. [2]Flow Cytometry Core Facility, Albert Einstein College of Medicine, New York, New York 10461, USA. [3]Ortho Biotech Oncology R&D, 145 King of Prussia Road, Radnor, Pennsylvania 19087, USA.

7 h after intravenous injection of Met-1 cells, a time point before significant interaction between the tumour and macrophages, and before extravasation of tumour cells[2]. Compared to control lungs, the recruitment of inflammatory monocytes to tumour-cell-challenged lungs increased markedly, with the ratio of inflammatory monocytes to resident monocytes increasing more than fivefold (Fig. 1c). However, this preferential recruitment of inflammatory monocytes was not observed after intravenous injection with PBS or latex beads, as controls for injection and particle lodgement, respectively (Supplementary Fig. 4e and data not shown). Consistent with this early recruitment of inflammatory monocytes, MAMs expressing high levels of CCR2 were preferentially recruited to lungs 36 h after tumour-cell inoculation[2]. However, B cells and T cells, including Foxp3$^+$ regulatory T (T_{reg}) cells, were not differentially recruited at this time (Supplementary Fig. 5a–c and data not shown). These data indicate that MAMs are derived from inflammatory monocytes that are specifically recruited early in the process of pulmonary metastasis, before other immune cells.

Distinct chemokine signals recruit inflammatory and resident monocytes[7], with inflammatory monocytes responding to CCL2 (refs 10, 11). Lung metastases of PyMT tumours express CCL2 homogeneously, in contrast to its heterogeneous expression in primary tumours (Supplementary Fig. 6a–d), and inflammatory monocytes have high levels of CCR2 expression, whereas resident monocytes do not (Supplementary Fig. 6e). The neutralization of CCL2 using a CCL2-specific antibody[13] markedly inhibited both the recruitment of inflammatory monocytes to lungs challenged with metastatic tumour cells (Fig. 1d) and the increase in the number of MAMs at the metastatic site (Supplementary Fig. 4f). Other CCR2-expressing leukocytes (a sub-population of T cells) and also T_{reg} cells were unaffected by anti-CCL2 antibody treatment in this model (Supplementary Fig. 5d). Furthermore, the preferential recruitment of inflammatory monocytes to the tumour-cell-challenged lung was completely abrogated during adoptive transfer of monocytes sorted from *Ccr2*-null mice (Supplementary Fig. 6f).

The pattern of human monocyte recruitment to tumours *in vivo* is unknown. To investigate this, human CD14$^+$CD16$^-$ inflammatory monocytes and CD14^{low}CD16$^+$ resident monocytes[9] were sorted from enriched CD14$^+$ cells from the peripheral blood of healthy donors (Supplementary Fig. 7a). 10^5 cells of each population were adoptively transferred into pairs of nude mice supplemented with recombinant human colony-stimulating factor 1 (CSF1), which is essential for the survival of monocytes and macrophages (Supplementary Fig. 7e). Human monocytes were quantified 18 h after adoptive transfer, using FACS analysis with an antibody against human CD45 (Supplementary Fig. 7b). In normal mice, after adoptive transfer of monocytes from the same donor, there were comparable numbers of human inflammatory monocytes and resident monocytes in the circulation and also recruited to the lung, but about twice the numbers of inflammatory monocytes compared to resident monocytes in the spleen (Fig. 1e, open bars). In mice given an intravenous injection of human MDA-MB-231-derived metastatic 4173 breast cancer cells[14] 7 h before monocyte transfer, the ratio of the two monocyte populations in blood and spleen was similar to that in normal mice, but the ratio of inflammatory monocytes to resident monocytes in the lungs increased more than sixfold (Fig. 1e). In established pulmonary metastases derived from orthotopically injected 4173 cells, inflammatory monocytes were also preferentially recruited, with a ratio fivefold higher than that in normal lungs (Supplementary Fig. 7d). Mouse inflammatory monocytes were also preferentially recruited to lungs challenged with 4173 cells (data not shown). Human inflammatory monocytes express CCR2, whereas resident monocytes express minimal levels of this receptor (Supplementary Fig. 7c). The neutralization of host CCL2 with an antibody against mouse CCL2 markedly reduced the recruitment of human inflammatory monocytes into lungs challenged with 4173 cells, without any change in the circulation or spleen (Fig. 1f). Treatment with an antibody specific to human CCL2 (ref. 15) also inhibited inflammatory monocyte recruitment (Supplementary Fig. 7f), indicating the importance of CCL2 from both the tumour and the target organ. This shows that human inflammatory monocytes respond to the same CCL2–CCR2 signalling as mouse cells for their specific recruitment during pulmonary metastasis.

To test the effect on metastatic potential of blocking the recruitment of inflammatory monocytes, we performed experimental metastasis assays with Met-1 cells in mice treated with anti-mouse CCL2 or with a control antibody shortly before the tumour-cell injection. Anti-CCL2 treatment reduced the total metastasis burden, owing to a markedly reduced number of metastasis nodules (Fig. 2a, b). An antibody specific to mouse CCL12, another ligand of mouse CCR2, had no effect on the metastasis of Met-1 cells (Supplementary Fig. 8). This indicates that the specific CCL2-mediated recruitment of inflammatory monocytes is critical for the pulmonary seeding of tumour cells.

Extravasation is a critical step for the metastatic seeding of tumour cells in the lung[2]. We used an intact-lung imaging system[16] to test the role of CCL2-recruited inflammatory monocytes in tumour-cell extravasation. *Csf1r–GFP* transgenic mice were injected intravenously with cyan fluorescent protein (CFP)-expressing Met-1 cells and analysed after 24 h. Quantification of three-dimensional reconstructed confocal images (Fig. 2c, d and Supplementary Movies 1 and 2) showed that the number of macrophages interacting directly with tumour cells was significantly reduced by anti-mouse CCL2 neutralizing antibody, compared with control antibody (Fig. 2e). Notably, tumour-cell extravasation was delayed and less efficient after the blocking of inflammatory monocytes (Fig. 2f). Tumour-cell extravasation involves crosstalk between tumour cells, endothelial cells, basement membrane and macrophages. In an *in vitro* trans-endothelial migration assay (Supplementary Fig. 9a)[17], the trans-endothelial migration of tumour cells was enhanced about fivefold by mouse bone-marrow-derived macrophages (BMDMs) located on the basolateral side of the endothelial monolayer. This effect was blocked by anti-mouse-CCL2 neutralizing antibody, but not by control antibody (Supplementary Fig. 9b). Tumour cells, BMDMs and endothelial cells all express CCL2, whereas only the macrophages express CCR2 (Supplementary Fig. 9c), indicating that only macrophages respond to the CCL2 chemokine signalling. In confirmation of this, macrophages from *Ccr2*-null mice were not capable of promoting trans-endothelial migration of tumour cells (Supplementary Fig. 9d). Notably, FACS-sorted inflammatory monocytes, but not resident monocytes, markedly promoted tumour-cell trans-endothelial migration and this was also inhibited by anti-mouse-CCL2 neutralizing antibody (Fig. 2g, h).

Total blockade of CCL2 (both mouse and human) inhibited spontaneous lung metastasis of orthotopically injected MDA-MB-231 cells (Fig. 3a). Ligands secreted by both the tumour cells and the host contributed to metastatic efficiency, because both anti-human and anti-mouse antibodies markedly inhibited the experimental metastasis of 4173 cells (Fig. 3b) without affecting tumour-cell proliferation *in vitro* (data not shown). This conclusion was also confirmed by knocking down *CCL2* using small interfering RNAs in 4173 cells: this markedly reduced lung colonization in experimental metastasis assays (Supplementary Fig. 10e, f). Consistent with this, a similar *Ccl2*-knockdown in Met-1 cells did not affect tumour-cell proliferation *in vitro*, but markedly inhibited the metastastic efficiency of the cells (Supplementary Fig. 10a–c). Trans-endothelial migration of 4173 cells *in vitro* was also promoted by human inflammatory monocytes and inhibited by neutralizing either human or mouse CCL2 with specific antibodies (Fig. 3c–e). These data indicate that CCL2 secreted by both the tumour cell and the target organ promotes tumour-cell extravasation and metastatic seeding via the recruitment of inflammatory monocytes. Consistent with the role of CCL2 synthesized by the microenvironment in the lung, bone metastases of MDA-MB-231 cells also recruit inflammatory monocytes and the inhibition of CCL2 inhibits metastatic progression. In contrast, liver metastases of Met-1 cells did not recruit inflammatory monocytes and CCL2 inhibition did not reduce metastasis (data not shown). Furthermore, CCL2 blockade 2 d after intravenous injection of MDA-MB-231 cells reduced the tumour burden in the lung and prolonged the

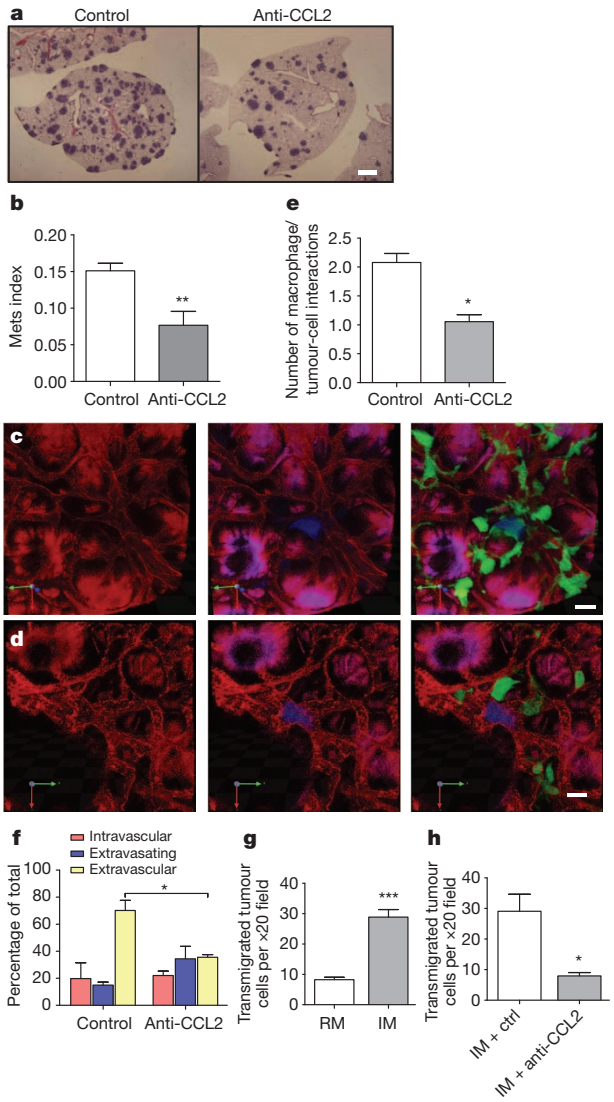

Figure 2 | CCL2-recruited monocytes promote metastatic seeding. **a**, Representative haematoxylin-&-eosin-stained sections showing Met-1 metastasis with control or anti-CCL2 antibody treatment. Scale bar, 1 mm. **b**, Met-1 metastasis (Mets) burden with or without antibody treatment. $n = 6$; **, $P = 0.006$. **c**, **d**, Representative snapshots of three-dimensional reconstructed confocal images of tumour cells (blue) and macrophages (green) in lung vasculature (red) 24 h after tail-vein injection of tumour cells into mice treated with control (**c**) or anti-mouse CCL2 (**d**) antibodies. Scale bar, 20 μm. Arrows define the dimensions of the figure. **e**, **f**, Numbers of interactions between macrophages and tumour cells (**e**) and tumour-cell extravasation (**f**) in mice with control or anti-mouse CCL2 antibody treatment. (**e**, $P = 0.0066$, and **f**, $P = 0.00163$, are based upon three-dimensional images of 15–20 tumour clusters per mouse, $n = 3$ mice per group.) **g**, Numbers of transmigrated Met-1 cells in the presence of resident monocytes or inflammatory monocytes. $n = 5$; ***, $P < 0.0001$. **h**, Numbers of transmigrated Met-1 cells in the presence of inflammatory monocytes, with antibody treatments. $n = 3$; *, $P = 0.0204$. All bars show mean + s.e.m.

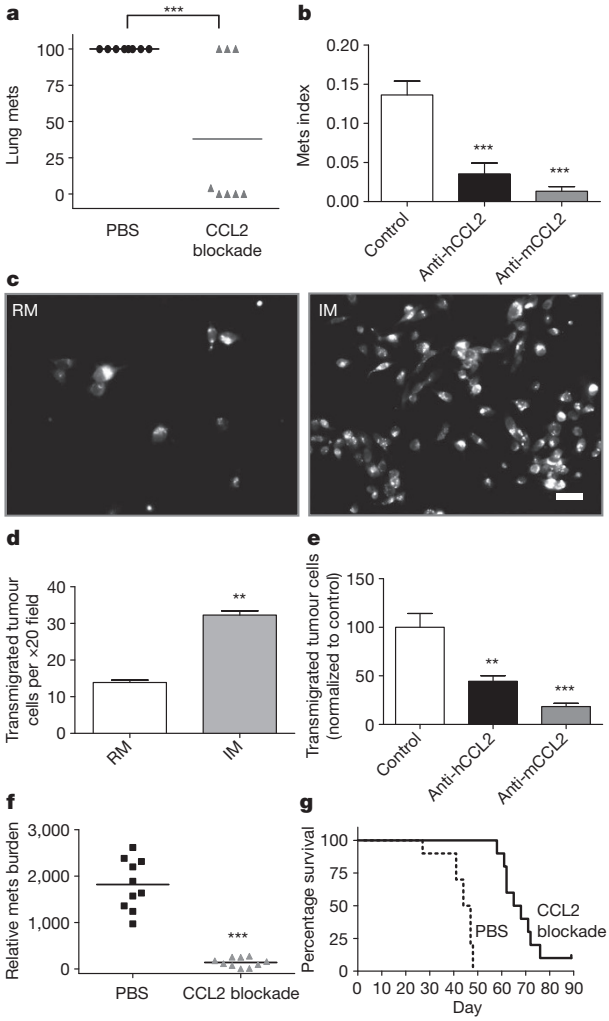

Figure 3 | CCL2 from both the tumour cell and the host promotes metastatic seeding. **a**, Numbers of spontaneous pulmonary metastases from orthotopic MDA-MB-231 tumours with total CCL2 blockade or control treatment. Bar shows the mean; $n = 8$ per group; ***, $P < 0.001$. **b**, Metastasis burden of intravenously injected 4173 cells with different antibody treatments. Bars show mean + s.e.m.; $n = 6$; ***, $P = 2.14 \times 10^{-5}$. **c**, Representative fluorescent micrographs of transmigrated human 4173 cells pre-stained with cell-tracker dye in the presence of inflammatory or resident monocytes. Scale bar, 20 μm. **d**, Numbers of transmigrated 4173 cells in the presence of inflammatory monocytes or resident monocytes. Bars show the mean + s.e.m. of three experiments with duplicates; **, $P = 0.0051$. **e**, Relative number of transmigrated 4173 cells in the presence of inflammatory monocytes with control, anti-human CCL2 or anti-mouse CCL2 antibodies, normalized to the average number with control antibody treatment, which is set to 100. Bars represent the mean + s.e.m. of five experiments with duplicates. One-way analysis of variance with Bonferroni's multiple comparison test; **, $P < 0.01$; ***, $P < 0.001$. **f**, **g**, CCL2 blockade starting from 2 d after intravenous injection of MDA-MB-231 cells significantly reduces the metastasis burden, as measured by real-time PCR of human Alu repeats, normalized to mouse β-actin, on day 22 (**f**, $n = 10$; ***, $P < 0.001$). CCL2 blockade also prolongs survival (**g**, $n = 10$, $P < 0.001$) compared to control treatment with PBS.

survival of mice, indicating the importance of continuous recruitment of inflammatory monocytes and their differentiation into MAMs for persistent metastatic growth (Fig. 3f, g).

To determine a mechanism for the effects of inflammatory monocytes on tumour-cell extravasation, we analysed the transcriptomes of resident and inflammatory monocytes[18]. Among the differentially regulated genes, vascular endothelial growth factor A (*Vegfa*) was highly expressed by inflammatory monocytes, a fact that we verified experimentally (Supplementary Fig. 11a). To ablate *Vegfa* conditionally in myeloid cells to test its role in the metastatic process, we generated a transgenic mouse expressing a tamoxifen-inducible Mer-iCre fusion protein driven by the *Csf1r* promoter, crossed with $Vegfa^{flox/flox}$ mice[19]. Inducible ablation of *Vegfa* was achieved in cultured BMDMs treated with 4-hydroxytamoxifen (Fig. 4a) and these *Vegfa*-null BMDMs were unable to promote the trans-endothelial migration of tumour cells and did not enhance permeability of the endothelial monolayer, a process important for metastasis[20], when compared to control BMDMs (Fig. 4b, c). *In vivo* injection of tamoxifen specifically ablated *Vegfa* in monocytes, without ablation in other circulating immune cells (Fig. 4d). This monocyte-specific depletion of VEGFA markedly inhibited the potential for experimental

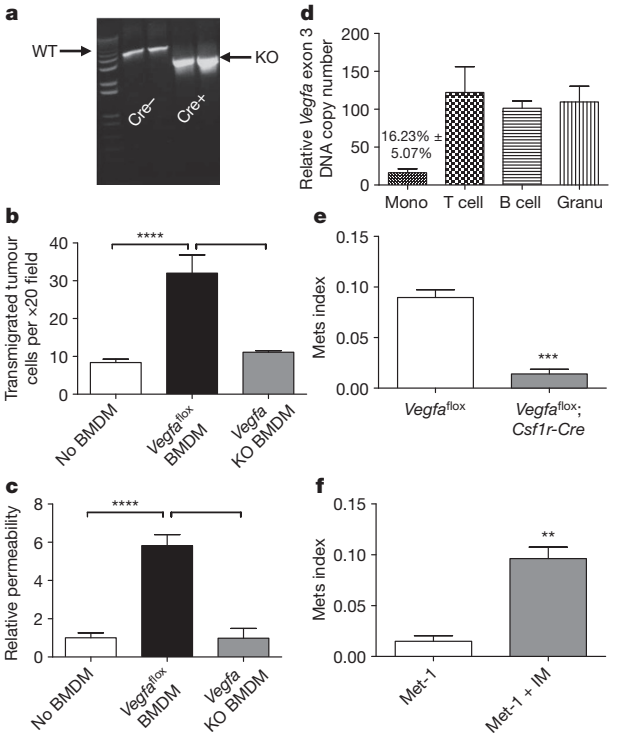

Figure 4 | Monocyte-specific ablation of *Vegfa* blocks pulmonary seeding. **a**, PCR of *Vegfa* exon 3 in BMDMs from $Vegfa^{flox/flox}$ mice, with or without the *Csf1r-Mer-iCre-Mer* transgene, treated with 4-hydroxytamoxifen. Wild-type (WT) and knockout (KO) bands are indicated. **b**, **c**, Numbers of trans-endothelial migrated Met-1 cells (**b**) and permeability of the endothelial monolayer to albumin (**c**), with no BMDMs, $Vegfa^{flox}$ BMDMs or *Vegfa*-knockout BMDMs. $n = 3$ with duplicates; **, $P < 0.01$ with analysis of variance. **d**, Relative copy number of *Vegfa* exon 3 in leukocytes from the peripheral blood of tamoxifen-treated $Vegfa^{flox/flox}$ *Csf1r-Mer-iCre-Mer* mice compared with $Vegfa^{flox/flox}$ mice. Mono, monocyte; granu, granulocyte. **e**, Met-1 Mets burden in $Vegfa^{flox/flox}$ mice with or without *Cre*, with the same tamoxifen treatment. $n = 6$; ***, $P = 0.0004$. **f**, Met-1 Mets burden in $Vegfa^{flox/flox}$ *Csf1r-Mer-iCre-Mer* mice with tamoxifen treatment, with or without co-injection of inflammatory monocytes. $n = 6$; **, $P < 0.0001$. All data are mean + s.e.m.

metastasis of Met-1 cells and reduced their seeding efficiency (Fig. 4e and Supplementary Fig. 11b). Adoptive transfer experiments indicated that *Vegfa*-null inflammatory monocytes infiltrate Met-1 lung metastases at a comparable level to $Vegfa^{flox}$ inflammatory monocytes, showing that VEGFA is not required for the recruitment of these cells (Supplementary Fig. 11c). Notably, co-injection of Met-1 cells and wild-type inflammatory monocytes into inducible macrophage-*Vegfa*-knockout mice restored the metastatic potential of tumour cells (Fig. 4f).

These experiments indicate that CCL2 synthesized by metastatic tumour cells and by the target-site tissue stroma is critical for the recruitment of a sub-population of CCR2-expressing monocytes that enhance the subsequent extravasation of the tumour cells. Mechanistically, this occurs at least in part through targeted delivery of molecules such as VEGFA that promote extravasation. Inflammatory monocytes are continually recruited by a CCL2-dependent mechanism and differentiate into macrophages that promote the subsequent growth of metastatic cells (Supplementary Fig. 1). These data, together with the clinical association of CCL2 overexpression in human cancers with poor prognosis (Supplementary Fig. 2), strongly argue for therapeutic approaches targeted against monocyte recruitment and function.

METHODS SUMMARY

The trafficking of monocytes into primary tumours and their metastases was studied by adoptive transfer of mouse ($Ly6c/Gr1^+$ or $Ly6c/Gr1^-$) monocytes or human ($CD14^+CD16^+$ and $CD16^-$) monocytes, using MMTV-PyMT autochthonous, human and mouse experimental metastasis models and human orthotopic tumour models. Monocytes and macrophages were recovered by enzymatic disaggregation of the tumours, followed by FACS analysis. To investigate mechanisms for monocyte recruitment and the effect of inhibition of this recruitment on metastasis, anti-mouse-CCL2 or anti-human-CCL2 antibodies or *Ccr2*-null mutant mice were used. To ablate *Vegfa* expression in monocytes, a myeloid-specific (*Csf1r* promoter), tamoxifen-inducible Cre-expressing strain was crossed with $Vegfa^{flox/flox}$ mice and gene ablation was induced by tamoxifen. The effect of monocyte depletion on tumour-cell extravasation using Met-1, an FVB PyMT-tumour-derived metastatic cell line, was determined using an *ex vivo* intact-lung imaging system and an *in vitro* extravasation assay.

Full Methods and any associated references are available in the online version of the paper at www.nature.com/nature.

Received 24 May 2010; accepted 19 April 2011.
Published online 8 June 2011.

1. Qian, B. Z. & Pollard, J. W. Macrophage diversity enhances tumor progression and metastasis. Cell **141,** 39–51 (2010).
2. Qian, B. *et al.* A distinct macrophage population mediates metastatic breast cancer cell extravasation, establishment and growth. *PLoS ONE* **4,** e6562 (2009).
3. Ueno, T. *et al.* Significance of macrophage chemoattractant protein-1 in macrophage recruitment, angiogenesis, and survival in human breast cancer. *Clin. Cancer Res.* **6,** 3282–3289 (2000).
4. Valkovic, T., Lucin, K., Krstulja, M., Dobi-Babic, R. & Jonjic, N. Expression of monocyte chemotactic protein-1 in human invasive ductal breast cancer. *Pathol. Res. Pract.* **194,** 335–340 (1998).
5. Saji, H. *et al.* Significant correlation of monocyte chemoattractant protein-1 expression with neovascularization and progression of breast carcinoma. *Cancer* **92,** 1085–1091 (2001).
6. Rhodes, D. R. *et al.* ONCOMINE: a cancer microarray database and integrated data-mining platform. *Neoplasia* **6,** 1–6 (2004).
7. Geissmann, F. *et al.* Blood monocytes: distinct subsets, how they relate to dendritic cells, and their possible roles in the regulation of T-cell responses. *Immunol. Cell Biol.* **86,** 398–408 (2008).
8. Geissmann, F. *et al.* Development of monocytes, macrophages, and dendritic cells. *Science* **327,** 656–661 (2010).
9. Geissmann, F., Jung, S. & Littman, D. R. Blood monocytes consist of two principal subsets with distinct migratory properties. *Immunity* **19,** 71–82 (2003).
10. Getts, D. R. *et al.* $Ly6c^+$ "inflammatory monocytes" are microglial precursors recruited in a pathogenic manner in West Nile virus encephalitis. *J. Exp. Med.* **205,** 2319–2337 (2008).
11. Palframan, R. T. *et al.* Inflammatory chemokine transport and presentation in HEV: a remote control mechanism for monocyte recruitment to lymph nodes in inflamed tissues. *J. Exp. Med.* **194,** 1361–1374 (2001).
12. Borowsky, A. D. *et al.* Syngeneic mouse mammary carcinoma cell lines: two closely related cell lines with divergent metastatic behavior. *Clin. Exp. Metastasis* **22,** 47–59 (2005).
13. Tsui, P. *et al.* Generation, characterization and biological activity of CCL2 (MCP-1/JE) and CCL12 (MCP-5) specific antibodies. *Hum. Antibodies* **16,** 117–125 (2007).
14. Minn, A. J. *et al.* Genes that mediate breast cancer metastasis to lung. *Nature* **436,** 518–524 (2005).
15. Carton, J. M. *et al.* Codon engineering for improved antibody expression in mammalian cells. *Protein Expr. Purif.* **55,** 279–286 (2007).
16. Al-Mehdi, A. B. *et al.* Intravascular origin of metastasis from the proliferation of endothelium-attached tumor cells: a new model for metastasis. *Nature Med.* **6,** 100–102 (2000).
17. Ma, C. & Wang, X.-F. *In vitro* assays for the extracellular matrix protein-regulated extravasation process. *CSH Protoc.* doi:10.1101/pdb.prot5034 (2008).
18. Swirski, F. K. *et al.* Identification of splenic reservoir monocytes and their deployment to inflammatory sites. *Science* **325,** 612–616 (2009).
19. Gerber, H. P. *et al.* VEGF is required for growth and survival in neonatal mice. *Development* **126,** 1149–1159 (1999).
20. Huang, Y. *et al.* Pulmonary vascular destabilization in the premetastatic phase facilitates lung metastasis. *Cancer Res.* **69,** 7529–7537 (2009).

Supplementary Information is linked to the online version of the paper at www.nature.com/nature.

Acknowledgements This work was supported by grants from the NIH to J.W.P. (NIH PO1 CA100324 and RO1 CA131270) and to the Albert Einstein Cancer Center Core (P30 CA 13330). We thank J. Massague for 4173 cells and N. Ferrara for the $Vegfa^{flox/flox}$ mice. We also thank P. Marsters for statistical analyses and M. Thompson, F. Shi, C. Ferrante, F. McCabe, H. Millar-Quinn and D. Wiley for discussions and technical assistance.

Author Contributions B-Z.Q., L.A.S. and J.W.P. conceived the ideas and designed the experiments. B-Z.Q., J.L., H.Z., T.K., J.Z., L.R.C. and E.A.K. performed the experiments. B-Z.Q., J.L., L.A.S. and J.W.P. analysed the data. B-Z.Q., L.A.S. and J.W.P. wrote the paper.

Author Information Reprints and permissions information is available at www.nature.com/reprints. The authors declare no competing financial interests. Readers are welcome to comment on the online version of this article at www.nature.com/nature. Correspondence and requests for materials should be addressed to J.W.P. (pollard@aecom.yu.edu).

METHODS

Animals. All procedures involving mice were conducted in accordance with National Institutes of Health regulations concerning the care and use of experimental animals. The study of mice was approved by the Albert Einstein College of Medicine and Ortho Biotech R&D Institute animal care and use committees. Transgenic mice expressing the Polyoma Middle T (PyMT) oncogene under the control of the mouse mammary tumour virus long terminal repeat (MMTV LTR) promoter were provided by W. J. Muller and were bred in-house. FVB (*Tg(Csf1r-EGFP)1Jwp*) mice have been previously reported to have the whole mononuclear phagocyte system labelled[2]. BL6 *Ccr2*^{tm1Ifc}/J mice were purchased from The Jackson Laboratory. The FVB macrophage-specific (*Csf1r* promoter), tamoxifen-inducible Cre-expressing *Tg(Csf1r-Mer-iCre-Mer)1Jwp* transgenic mouse strain was generated and crossed with *Vegfa*$^{flox/flox}$ mice (gift from N. Ferrara). Knockout of *Vegfa* in myeloid cells was induced by daily subcutaneous injection of 3 μg tamoxifen per mouse for 2 d, before sorting for blood leukocytes or tumour-cell injection.

Metastasis assay. Eight-week-old FVB females and six-week-old female nude mice were used for lung experimental-metastasis assays with intravenous injection of 5×10^5 Met-1 cells or 10^6 MDA-MB-231-derived LM2 human breast cancer cells, 4173 (ref. 14), respectively. If not otherwise specified, all animals were killed 2 weeks after intravenous injection of Met-1 cells or 4 weeks after injection of human tumour cells, for optimal metastatic burden. In experimental metastasis assays, antibodies were given at 10 mg kg^{-1} body weight via intraperitoneal injection 3 h before tumour-cell injection, for single treatments, or twice a week thereafter for prolonged treatments, if not otherwise specified. For paraffin sections, lungs were injected with 1.2 ml of 10% neutral buffered formalin by tracheal cannulation to fix the inner airspaces and inflate the lung lobes. Lungs were excised and fixed in formalin overnight. A precise stereological method[21] with modification was used for quantification of lung metastases. Briefly, paraffin-embedded lungs were systematically sectioned through the entire lung with one 5 μm section taken in every 0.5 mm of lung thickness. All sections were stained with haematoxylin and eosin and images were taken using a Zeiss SV11 microscope with a Retiga 1300 digital camera and analysed using ImageJ[22]. The Mets index is the total volume of metastases normalized to total lung volume and Mets number is the number of metastasis nodules per mm^2 of lung area. Real-time PCR quantification of the burden of human tumour cells was performed as reported previously, using human-specific primers[23]. For spontaneous lung metastasis, 2.5×10^6 parental MDA-MB-231 cells or 10^6 derived LM2 4173 tumour cells were orthotopically injected into the inguinal mammary gland of SCID beige or nude mice, respectively. Anti-mouse CCL2 and CCL12 (ref. 23) and anti-human CCL2 (ref. 15) antibodies neutralize only their respective target molecules and were provided by Ortho Biotech Oncology together with the control antibody. In spontaneous metastasis assays, antibody treatment began on day 3 after tumour-cell intra-mammary-gland injection and continued twice a week thereafter, with each antibody used at 20 mg kg^{-1} body weight. When each group reached a mean primary-tumour volume of ~1,000 mm^3, the mice were killed. Lungs were perfused with India ink and placed in Fekete's solution. Lung metastases were counted in a blinded fashion. All *in vivo* experiments were at least two independent experiments with 3–10 mice for each group.

Adoptive transfer. CD115$^+$ F4/80$^+$ CD11b$^+$ Ly6c1/Gr1$^+$ and Ly6c1/Gr1$^-$ bone-marrow monocytes were sorted from FVB Csf1r-EGFP mice and adoptively transferred into FVB mice. 10^5 of either cell type were transferred into mice bearing mammary tumours and/or pulmonary metastases. Monocytes were sorted from *Ccr2*-null mutant mice using the same protocol and were labelled with CellTracker (Invitrogen) following the manufacturer's instructions, before adoptive transfer into nude mice. Fresh human CD14$^+$ peripheral monocytes were purchased from All Cells LLC. 10^5 CD14$^+$CD16$^-$ and CD14$^+$CD16$^+$ cells were FACS-sorted and intravenously transferred into nude mice supplemented with 2×10^6 units of recombinant human CSF1 via subcutaneous injection. In the indicated experiments, specified antibodies were given at 10 mg kg^{-1} body weight 3 h before adoptive transfer of monocytes.

FACS analysis and antibodies. For FACS analysis, lungs or whole mice were perfused thoroughly with cold PBS before cell collection, then lungs were minced on ice and digested with an enzyme mix of Liberase and Dispase (Invitrogen). Blood was drawn by cardiac puncture. Red blood cells were removed using RBC lysis buffer (eBioscience). Cells were blocked using anti-mouse CD16/CD32 antibody (eBioscience) for mouse cells, or 10% goat serum for human cells, before antibody staining. Antibodies against mouse antigens were: CD45 (30-F11), CD11b (M1/70), Gr1 (RB6-8C5), CD115 (AFS98) and Foxp3 (FJK-16 s; all from eBioscience); CD3 (145-2C11) and Ly6c1 (HK1.4; both from Biolegend); CD25 (PC61), CD62L (MEL-14), IL4Ra (mIL4R-M1), CD4 (GK1.5), CD8a (53-6.7) and Ly6G (1A8; all from BD Pharmingen) and F4/80 (Cl:A3-1; AbD Serotec). Antibodies against human antigens were: CD14 (Tük4) and CD16 (3G8; both from Invitrogen), CD45 (HI30; BioLegend) and CCR2 (48607; R&D Systems). FACS analysis was performed on a LSRII cytometer (BD Biosciences) and data were analysed using Flowjo software (TreeStar). Gating of single cells using FSC/W and SSC/W and exclusion of dead cells with DAPI staining were performed routinely during analysis. Mouse CCL2 was stained using the specific antibody R-17 (Santa Cruz) after a standard immunohistochemistry protocol.

Cell culture and *in vitro* extravasation assay. All cells were cultured in Dulbecco's modified Eagle's medium (DMEM), supplemented with 10% fetal bovine serum (FBS). The extravasation assay was performed as previously described[17,24] with modifications. Briefly, 2×10^4 endothelial cells (3B-11, ATCC) were plated into the upper chamber of a GFR matrigel invasion chamber (BD Biosciences) in DMEM with 10% (v/v) FBS. A monolayer was formed in 2 d and was verified by microscopy. 10^4 BMDMs or FACS-sorted monocytes were loaded to the basolateral side of the insert and put into a plate-well with DMEM, 10% FBS and 10^4 units ml^{-1} CSF1 to allow attachment. *Vegfa*-knockout BMDMs derived from *Csf1r-Mer-iCre-Mer:Vegfa*$^{flox/flox}$ mice were induced by treating the cells with 1 μM 4-hydroxyltamoxifen for 7 d after isolation of bone marrow. 2×10^4 Met-1 cells stained with CellTracker CMRA (Invitrogen) were loaded into the insert with DMEM in 0.5% (v/v) FBS and 10^4 units ml^{-1} CSF1. CCL2-neutralizing antibody and control antibody were used at 5 ug ml^{-1}, applied to both sides of the insert. Plates were incubated under normal tissue-culture conditions for 36–48 h before being fixed with 1% (w/v) paraformaldehyde. Tumour-cell trans-endothelial migration was quantified by counting the number of cells that migrated through the insert under a fluorescent microscope (6–10 randomly-selected fields in each insert) and was expressed as cell number per ×20 field, if not otherwise specified. The permeability assay was performed by loading 4% (w/v) bovine serum ambumin labelled with Evan's blue into the upper chamber with a pre-formed endothelial monolayer of 3B-11 cells and measuring the absorption of the phenol-red-free medium in the lower chamber at 650 nm after a 30-min incubation in normal culturing conditions. All *in vitro* experiments were at least three independent experiments with duplicate or triplicate measures.

Molecular biology. To knockdown *Ccl2* in Met-1 cells, a 97-mer oligo containing a small hairpin RNA (shRNA) that targets the *Ccl2* mRNA sequence from nucleotide 166 was cloned into the miR30 context in the retroviral vector P2GM[25]. To knockdown *CCL2* in 4173 cells, a 97-mer oligo containing a shRNA targeting the human *CCL2* mRNA sequence from nucleotide 255 was cloned into the miR30 context in the same vector. For real-time PCR of mouse *Ccl2* expression, primers CCCAATGAGTAGGCTGGAGA and AAAATGGATC CACACCTTGC were used, and for *Ccr2*, primers CCTGCAAAGACCAGAAG AGG and GTGAGCAGGAAGAGCAGGTC. All real-time PCR was performed on an MJ Research DNA Engine 2 Opticon real-time PCR machine using SYBR master mix (Invitrogen). Primers used were: mouse *Ccl2* primers GTTGGC TCAGCCAGATGCA and AGCCTACTCATTGGGATCATCTTG; mouse *Ccr2* TTTGTTTTTGCAGATGATTCAA and TGCCATCATAAAGGAGCCAT; mouse *Plau* ACAGATAAGCGGTCCTCCAG and GCCCCACTACTATGGCTC TG; mouse *Vegfa* AATGCTTTCTCCGCTCTGAA and GCTTCCTACAGCACA GCAGA; mouse *Vegfa* exon 3 ACATCTTCAAGCCGTCCTGT and CTGCAT GGTGATGTTGCTCT; human *CCL2* AGGTGACTGGGGCATTGAT and GCCTCCAGCATGAAAGTCTC. To verify mouse *Vegfa* exon 3 knockout, primers that flank this exon, GCTGCACCCACGACAGAAGG and TGAGGTT TGATCCGCATGAT, were used.

***Ex vivo* whole-lung imaging.** A well-established intact-lung microscopy technique[16,26] was applied to observe tumour cells, macrophages and blood vessels in mouse lungs. CFP-expressing Met-1 cells, prepared by retrovirus infection of a CMV-promoter CFP vector, were injected intravenously into the tail vein of each mouse. At the times indicated, mice were anaesthetized and injected with 10 μg AlexaFluor-647-conjugated anti-mouse CD31 antibody (BioLegend). Five minutes later, the mouse was put under artificial ventilation through tracheal cannulation. The lung was cleared of blood by gravity perfusion through the pulmonary artery with artificial medium (Kreb-Ringer bicarbonate buffer with 5% dextran and 10 mmol l^{-1} glucose (pH 7.4)). The heart–lung preparation was dissected en bloc and placed in a specially designed plexiglass chamber with a port to the artificial cannula. The lung rested on a plexiglass window at the bottom of the chamber with the posterior surface of the lung touching the plexiglass. The lung was ventilated throughout the experiment with 5% CO_2 in medical air and perfused by gravity perfusion except during imaging. Three to five animals were imaged for each time point and 10–20 unrelated fields were imaged for each animal.

Images were collected with a Leica TCS SP2 AOBS confocal microscope (Mannheim) with ×60 oil-immersion optics. Laser lines at 458 nm, 488 nm and 633 nm for excitation of CFP, GFP and AF647, respectively, were provided by an Ar laser and a HeNe laser. Detection ranges were set to eliminate crosstalk between fluorophores. Three-dimensional reconstruction was performed using Volocity (Improvision Inc.).

Statistical analysis. Statistical analysis methods were the standard two-tailed Student's *t*-test for two data sets and ANOVA followed by Bonferroni/Dunn post

hoc tests for multiple data sets using Prism (GraphPad Inc.), except for human-monocyte transfer with antibody treatment, where a paired *t*-test was used because of variations among different donors. For the spontaneous-metastasis assay of MDA-MB-231 cells, percentage differences in numbers of lung metastases were compared between groups using parametric survival regression methods, with metastasis counts of more than 100 considered censored at 100. *P* values of less than 0.05 were deemed significant.

21. Nielsen, B. S. *et al.* A precise and efficient stereological method for determining murine lung metastasis volumes. *Am. J. Pathol.* **158,** 1997–2003 (2001).
22. Abramoff, M. D., Magelhaes, P. J. & Ram, S. J. Image processing with ImageJ. *Biophotonics Int.* **11,** 36–42 (2004).
23. Havens, A. M. *et al.* An *in vivo* mouse model for human prostate cancer metastasis. *Neoplasia* **10,** 371–380 (2008).
24. Brandt, B. *et al.* 3D-extravasation model — selection of highly motile and metastatic cancer cells. *Semin. Cancer Biol.* **15,** 387–395 (2005).
25. Stern, P. *et al.* A system for Cre-regulated RNA interference *in vivo*. *Proc. Natl Acad. Sci. USA* **105,** 13895–13900 (2008).
26. Im, J. H. *et al.* Coagulation facilitates tumor cell spreading in the pulmonary vasculature during early metastatic colony formation. *Cancer Res.* **64,** 8613–8619 (2004).